# Imaging the mountainless root of the 1.8 Ga Cheyenne belt suture and clues to its tectonic stability

Jason A. Crosswhite
Eugene D. Humphreys
Department of Geological Sciences, 1272 University of Oregon, Eugene, Oregon 97403, USA

**ABSTRACT**

**Receiver-function analysis across the Cheyenne belt, an Archean–Proterozoic suture, images a 100-km-wide zone of 50–60-km-thick crust. This thick crust is thought to be a remnant from the original 1.8 Ga suturing event. The thick and presumably buoyant crust is remarkable in that it is not associated with a large topographic or gravitational anomaly, suggesting isostatic balance and a high-density mass at depth to compensate the crustal root. These features could account for the lithosphere's long-term stability. The presence of eclogite below the crustal root is a likely source for the high-density mass, as it would not produce a seismically unusual Moho, yet it would provide the required excess mass.**

**Keywords:** seismic discontinuities, seismic studies, suture zones, isostasy, Cheyenne belt.

## INTRODUCTION

Accretion and suturing of crust are the primary means of continental growth and the creation of continental fabric. Precambrian sutures, in particular, record continental formation and growth when processes may have differed from those occurring more recently. Starting ca. 1.8 Ga, most of the southwestern United States formed by Proterozoic accretion of active arcs onto the 3.2 Ga Wyoming craton along the south-dipping Cheyenne belt suture. That this assembly has been stable and has successfully avoided rifting ever since suggests that accretion resulted in low values of gravitational potential energy and little rifting potential.

To look at the deep structure of the Cheyenne belt, we back-projected teleseismic P-to-S conversions with the method of receiver-function stacking to produce images of crustal structure across the Cheyenne belt.

## DATA

Our study used two arrays of seismometers that were deployed at various times starting in August 1997 and ending July 1998 (Fig. 1). Arrays were located with special emphasis on the Cheyenne belt. The Deep Probe array consisted of ~40 broadband and high-frequency seismometers deployed for six months along a 450 km line. The Lodore array was a relatively dense, two-dimensional deployment of 33 broadband seismometers for 1 yr.

The 48 very good events ($m_b \gtrsim 5.9$) from the Lodore array and 38 usable events ($m_b \gtrsim 5.1$) from the Deep Probe array were distributed with roughly equal numbers arriving from the south and north, illuminating structure well.

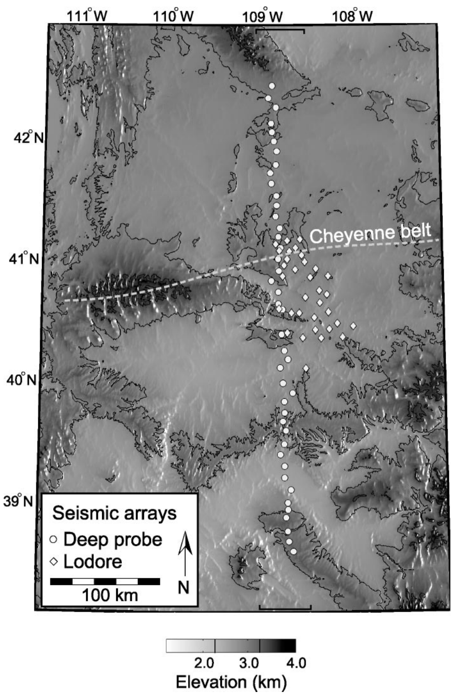


**Figure 1. Relief map showing seismic stations used in this study. Dashed line shows inferred location of 1.8 Ga Cheyenne belt suture (Karlstrom and Houston, 1984; Karlstrom and Humphreys, 1999) between Archean crust to north and Proterozoic crust to south. Brackets to north and south of arrays represent horizontal distance over which topography and gravity were averaged for profiles in Figure 3.**

## METHODOLOGY

Teleseismic waveforms were analyzed by using receiver-function analysis (Langston, 1977). This method uses P-to-S converted waves generated by interfaces beneath a seismometer to estimate interface depth and seismic impedance contrast. Stacking back-projections of receiver functions along their ray paths produces images of interface structure (Dueker and Sheehan, 1997). Receiver-function waveforms (e.g., Fig. 2) were calculated by using standard methods. Specific details of waveform analysis include rotation into ray coordinates (P, SV, and T) (Vinnik, 1977), multiple taper deconvolution (Park and Levin, 2000), and forming a common source function by stacking the set of an event's vertical P components (Langston and Hammer, 2001).

Receiver functions were then distributed along their ray paths, segregated into bins, and averaged within each bin by using an inversion method similar to that of Sheehan et al. (2000) to obtain an estimate of impedance contrast across that bin. We modified the method to include weighting by the variance of presignal noise and a sharing of data between adjacent bins. Stacking parameters are given in Table 1.

Ray paths were calculated using a one-dimensional P-wave velocity structure derived from results of the Deep Probe active-source experiment (Snelson et al., 1998), to which we have incorporated sedimentary basins from the compilation of Woodward (1988). To obtain an initial S-wave velocity structure, we used $V_P/V_S$ ratios of 1.77 and 2.0 for the crust and sediment, respectively. Moveout calculations, which compute the arrival time of P-to-S conversions, used these $V_P$ and $V_S$ velocity structures (Gurrola et al., 1994). The results are shown in Figure 3.

We then apply the method of Zhu and Kanamori (2000) to obtain improved estimates of $V_P/V_S$ and crustal thickness. This method searches over many values of $V_P/V_S$ and Moho depth to find the specific values where the direct Moho P-to-S arrival and the Moho P and S

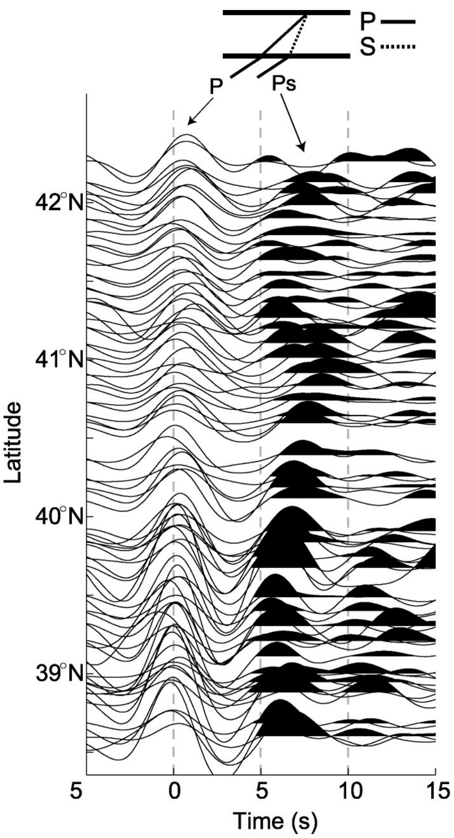


**Figure 2. Example receiver functions for one earthquake. Top diagram represents ray paths in crust. Strong arrivals between 5 and 10 s are P-to-S conversions (Ps) from Moho. Relatively late arrivals between 40° and 41°N are indicative of relatively thick crust.**

TABLE 1. STACKING PARAMETERS USED TO CREATE FIGURE 3

| Array | Bin length (km) | Bin depth (km) | Horizontal share (bins) | Vertical share (bins) | *a* | *f* (Hz) |
|---|---|---|---|---|---|---|
| Lodore | 3 | 1 | 3 | 1 | 2.5 | 0.067 |
| Deep Probe | 5 | 1 | 3 | 1 | 2.0 | 0.067 |

*Note*: Sharing distances are half widths measured in bins. Receiver functions were filtered with a low-pass Gaussian filter using the parameter *a* and a Butterworth high-pass filter with corner frequency *f*. The frequency of the low-pass corner is approximately half of *a*.

reverberations are most consistent with each other (e.g., Fig. 4). The method was modified with a second-root stack to average the values for each arrival. Table 2 indicates specific Moho depths and $V_P/V_S$ estimates derived from this analysis, and these depths are overlain in Figure 3.

The largest error in interface depth estimate is due to uncertainty in $V_P/V_S$ (Zhu and Kanamori, 2000), which trades off with depth. Assuming the estimated values of $V_P/V_S$ (Table 2) represent the range of $V_P/V_S$ in the area, we find the uncertainties in Moho depth imaged in Figure 3 to be $\sim\pm5$ km; the uncertainty in depth estimated with the Zhu and Kanamori (2000) grid search is significantly less.

**RESULTS**

Figure 3 shows the structure imaged beneath the arrays shown in Figure 1. Figure 3 is a composite, made of an image derived from the Deep Probe array overlain by a more resolved image below the Lodore array (the obscured structure from the Deep Probe image is similar to and consistent with the Lodore image). The Moho is imaged clearly as a band of high positive amplitude at depths of 40–60 km.

Our images are consistent with previous active and passive seismic results (Keller et al., 1998; Snelson et al., 1998), as well as with models derived from mantle xenoliths (Eggler et al., 1987). Newly imaged features include a zone of very thick crust south of the Cheyenne belt, a generally south-dipping set of conversions within the thick crust, and a step in crustal thickness ~150 km south of the suture, near the Uncompahgre uplift.

In a study similar to ours, Poppeliers (2000) used the data from the Lodore array to image the Cheyenne belt with receiver functions. Their image of the crust beneath the Lodore array is similar to ours, although there are structural and interpretive differences. These differences result primarily from the advantage provided us by the inclusion of Deep Probe data, which allowed us to follow the Moho unambiguously from the far field, where it is well understood, across the Cheyenne belt. In doing so, it is clear that the ~60-km-deep interface near the Cheyenne belt suture is continuous with the Moho away from the suture, which together define a rather continuous Moho.

**DISCUSSION**

The most distinct and peculiar feature imaged is the localized depression of the Moho directly south of the Cheyenne belt. The maximum crustal thickness of ~60 km falls outside two standard deviations from the global distribution (Christensen and Mooney, 1995), making it some of the thickest crust in North America.

Several tectonic events could be responsible for creating this thick crust: the 1.8 Ga suturing event, a 1.4 Ga episode of regional ano-

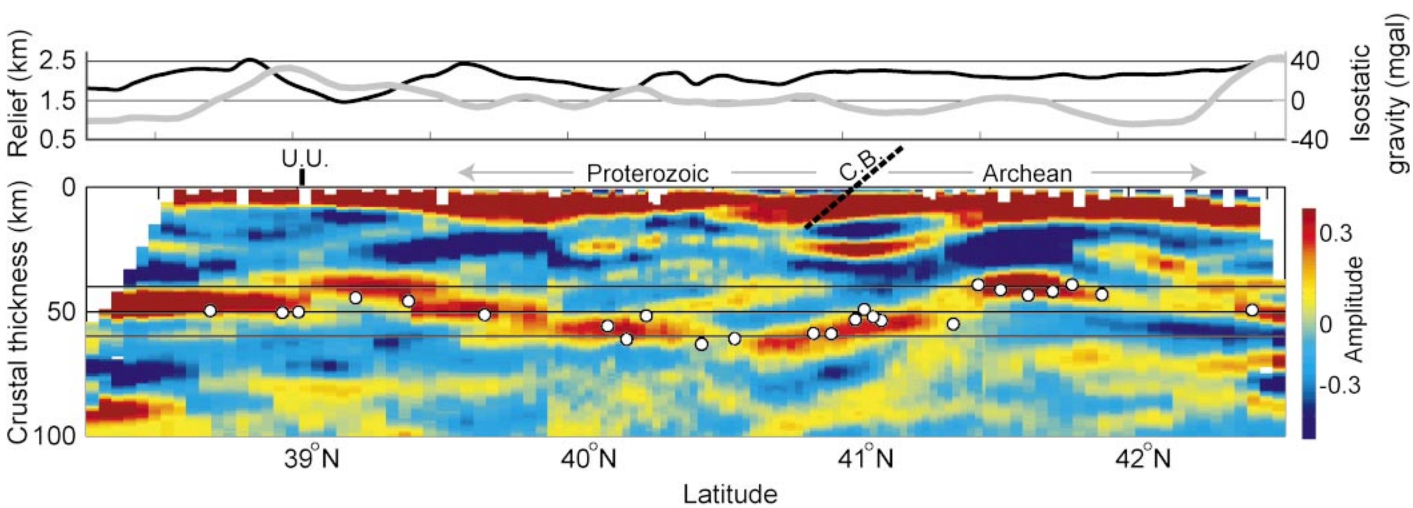


**Figure 3. Top plot shows average topographic (black) and isostatic gravity (gray) profiles along line of our investigation. Bottom is composite image of crust from common-conversion-point stacking, with no vertical exaggeration. (See Table 1 for stacking parameters.) Moho is imaged clearly as band of high positive amplitude (red) at depths of 40–60 km. Crust is thicker than 50 km from Cheyenne belt suture (C.B.) to ~100 km south (~40°N) and attains thickness of slightly more than 60 km 25 km south of suture. There is ~5 km Moho offset associated with Uncompahgre uplift (U.U.). White dots represent crustal thickness determined from method of Zhu and Kanamori (2000).**

rogenic magmatism, continental rifting ca. 500 Ma, the late Paleozoic Ancestral Rockies orogeny, and the 80–40 Ma Laramide orogeny. Regionally, the widespread 1.4 Ga magmatic event is not associated with crustal thickening, and there are no indications of unusual activity in our study area at that time. Although the Ancestral Rockies orogeny created the Uncompahgre uplift at the southern end of our line array, it did not affect the crust near the suture. The rifting ca. 500 Ma would have thinned the crust, not thickened it. This leaves either the original suturing or the Laramide orogeny as likely causes. In our field area, Laramide shortening of ~13 km (Hansen, 1984) is associated with the creation of the Uinta Mountains, and the faults that accommodated shortening are thought to originate near 20 km depth (Erslev, 1993). Assuming Airy isostasy, a preshortening crustal thickness of ~50 km, and standard crust and mantle densities, Laramide shortening would approach only 50% of the cross-sectional area necessary to explain the ~2900 km$^2$ crustal root. Therefore, the original suturing event is thought to be responsible for most of the crustal thickening. Because postcollisional rifting predicted by the Wilson cycle (Wilson, 1966) did not extend this suture (Karlstrom and Humphreys, 1999), this origin for the thick crust is not unexpected.

The seismic impedance contrast that we resolve is typical of Moho values, and because seismic impedance tends to scale directly with density contrast (Christensen and Mooney, 1995), a normal density contrast across the Moho is implied. If this is true, a large mountain range should exist in isostatic response to the locally thickened buoyant crust, and such a range clearly does not exist (Figs. 1 and 3). Even if the lithosphere were quite strong, e.g., with a flexural wavelength of ~400 km (as inferred by Lowry and Smith, 1995), a topographic swell ~200 km wide and 1 km high should be buoyed up by the imaged crustal root. The absence of upwarp implies that there is no significant buoyancy associated with the imaged Moho downwarp.

To look more closely at this surprising result, we examined the isostatic gravity field from this area (Figs. 3 and 5). If a relatively rigid lithosphere prevents local upwarping by holding down the crustal root, then a prominent isostatic gravity low would be observed with a magnitude similar to that observed over the individual Rocky Mountain uplifts (Fig. 5), but of opposite sign. Isostatic gravity is remarkably featureless along the line of our investigation. This gravity result corroborates the conclusion made considering the topography: there is no significant buoyancy anomaly associated with the imaged Moho downwarp.

The lack of an isostatic gravity anomaly not only indicates isostatic balance, it also indicates that the density moment (Fleitout and Froidevaux, 1982) is low (i.e., only a small vertical separation between any positive and negative compensating mass anomalies). Under normal conditions, the large density moment of locally thickened crust produces a considerable amount of gravitational potential energy and associated rifting potential. The crustal root beneath the Cheyenne belt appears, however, to have been stable over long periods of time. Thus, in spite of seismic evidence for a buoyant root, the absence of any

TABLE 2. CRUSTAL THICKNESS AND $V_P/V_S$

| Latitude (°N) | Crustal thickness (km) | $V_P/V_S$ |
|---|---|---|
| 42.45 | 49.28 | 1.72 |
| 41.90 | 42.97 | 1.82 |
| 41.80 | 39.13 | 1.80 |
| 41.73 | 41.87 | 1.77 |
| 41.64 | 43.24 | 1.72 |
| 41.54 | 41.18 | 1.75 |
| 41.46 | 39.13 | 1.86 |
| 41.37 | 54.90 | 1.67 |
| 41.11 | 53.53 | 1.79 |
| 41.08 | 52.02 | 1.89 |
| 41.05 | 49.00 | 1.90 |
| 41.02 | 53.12 | 1.82 |
| 40.93 | 58.88 | 1.73 |
| 40.86 | 58.74 | 1.79 |
| 40.58 | 60.80 | 1.85 |
| 40.46 | 62.99 | 1.66 |
| 40.37 | 61.07 | 1.73 |
| 40.26 | 51.61 | 1.89 |
| 40.19 | 61.07 | 1.68 |
| 40.12 | 55.72 | 1.77 |
| 39.68 | 51.20 | 1.78 |
| 39.40 | 45.71 | 1.71 |
| 39.21 | 44.34 | 1.70 |
| 39.01 | 49.96 | 1.70 |
| 38.95 | 50.24 | 1.69 |
| 38.69 | 49.55 | 1.73 |

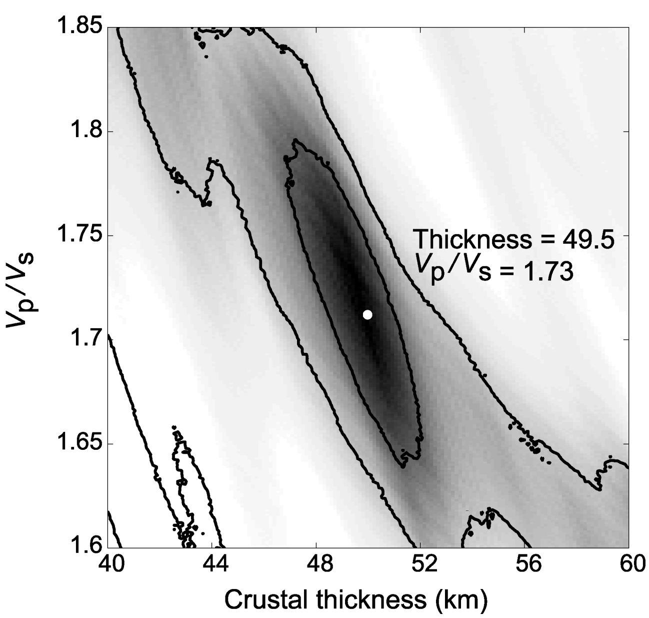


**Figure 4. Example of crustal thickness vs. $V_P/V_S$ stack for one seismic station. Each crustal thickness-$V_P/V_S$ point is formed by weighted sum of amplitudes from direct P-to-S conversion and its reverberations at times predicted for that point. Highest amplitude occurs where direct P-to-S arrival and crustal reverberations are most consistent. Skewed orientation of maximum reflects crustal thickness-$V_P/V_S$ tradeoff.**

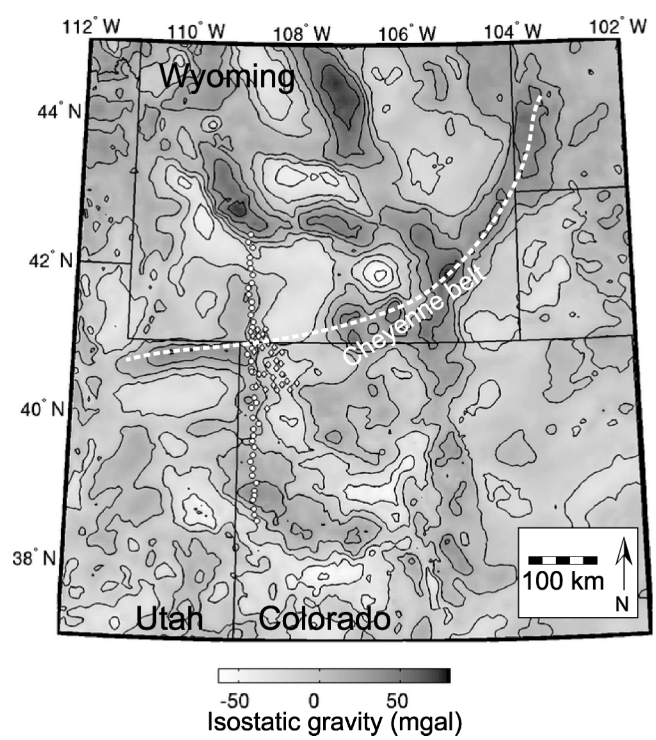


**Figure 5. Isostatic residual gravity (Simpson et al., 1986). Large positive anomalies delineate Rocky Mountain uplifts in Wyoming. No large gravity anomaly is apparent in area of thickened crust south of Cheyenne belt.**

significant gravitational anomaly and the long-term stability of the area lead us to conclude that the root is not and has not been a concentration of significant amounts of potential energy, and that any mass excess that is compensating the root is near to the root.

There are several ways a high-density mass excess could be rendered seismically undetectable. Structure having gradational boundaries at the wavelengths used in our investigation (i.e., with a structural transition $\gtrsim$15 km) would not be imaged well. Another possibility is that the mass anomaly is not a seismic anomaly, thereby making it seismically transparent. Eclogite would be a strong candidate for such a mass; its density is 200–250 kg/m$^3$ greater than upper mantle density, yet its seismic velocity is very similar to that of upper mantle. A likely source for the eclogite necessary for mass balance would be oceanic crust incorporated into the lithosphere during suturing, now stable below the basalt-to-eclogite phase transition at ~60 km depth. Support for this possibility is provided by the well-resolved increase of crustal $V_P/V_S$ (Table 2) in the vicinity of the suture. Generally, $V_P/V_S$ increases with the mafic content of rock (Christensen and Mooney, 1995), implying a mafic, possibly oceanic, lower crust. The deeper extension of this material could be the eclogite whose presence we infer.

These results are not without precedent. Seismic studies in the Bothnian Bay near Finland show a well-preserved, 42–48-km-thick, 1.89 Ga suture, complete with remnant oceanic crust (Dahl-Jensen et al., 1990). One of the more compelling examples is that of the Redbank deformed zone of central Australia (Goleby et al., 1989). Here a crustal-scale thrust fault offsets and imbricates the mantle, creating a structure that is seemingly out of isostatic equilibrium, yet has remained stable for more than 360 m.y. Similarly, the Urals were formed during suturing and have a crustal root that is much larger than would be inferred from their elevation alone (Thouvenot et al., 1995), suggesting high-density compensation at depth.

These observations lead to several broad conclusions. First is the important dynamic role of compensating high-density mantle. With the aid of deep compensating density structure, sutures can resist modification and survive through long periods of geologic time. Also, without accompanying topography or large gravity anomaly, these structures may be difficult to detect. In this matter, the low frequency waves used in teleseismic seismology are ideal, and initiatives such as the continental-scale USArray seismic deployment should allow us to map out and better understand these features. These results emphasize the importance of mantle density structure in the isostatic balance of the western United States. It has long been known that much of the Rockies have no roots (e.g., Sheehan et al., 1995); now we know that some of our roots do not have mountains. Only by looking at deep structure can we form the complete picture.

**REFERENCES CITED**


Christensen, N.I., and Mooney, W.D., 1995, Seismic velocity structure and composition of the continental crust: A global view: Journal of Geophysical Research, v. 100, p. 9761–9788.

Dahl-Jensen T., Hobbs, R.W., Klemperer, S.L., Matthews, D.H., Snyder, D.B., Long, R., Matthews, T., Blundell, D.J., Lund, C.-E., Palm, H., Pedersen, L.B., Roberts, R.G., Elming, S-Å., Heikkinen, P., Korhonen, H., Luosto, U., Hjelt, S-E., Komminaho, K., Yliniemi, J., Meissner, R., Sadowiak, P., Weyer, T., Dickmann, T., Flueh, E.R., Berthelsen, A., Thybo, H., Balling, N., and Nørmark, E., 1990, Evidence for early Proterozoic plate tectonics from seismic reflection profiles in the Baltic shield: Nature, v. 348, p. 34–38.

Dueker, K.G., and Sheehan, A.F., 1997, Mantle discontinuity structure from midpoint stacks of converted P to S waves across the Yellowstone hotspot track: Journal of Geophysical Research, v. 102, p. 8313–8327.

Eggler, D.H., Meen, J.K., Welt, F., Dudas, F.O., Furlong, K.P., McCallum, M.E., and Carlson, R.W., 1987, Tectonomagmatism of the Wyoming province, *in* Drexler, J.W., and Larson, E.E., eds., Cenozoic volcanism in the southern Rocky Mountains revisited: A tribute to Rudy C. Epis—Part 3: Colorado School of Mines Quarterly, v. 83, no. 2 , p. 25–40.

Erslev, E.A., 1993, Thrusts, back-thrusts, and detachment of Rocky Mountain foreland arches, *in* Schmidt, C.J., et al., eds., Laramide basement deformation in the Rocky Mountain foreland of the Western United States: Geological Society of America Special Paper 280, p. 339–357.

Fleitout, L., and Froidevaux, C., 1982, Tectonics and topography for a lithosphere containing density heterogeneities: Tectonics, v. 1, p. 21–56.

Goleby, B.R., Shaw, R.D., Wright, C., Kennet, B.L.N., and Lambeck, K., 1989, Geophysical evidence for ‘thick-skinned’ crustal deformation in central Australia: Nature, v. 337, p. 325–330.

Gurrola, H., Minster, J.B., and Owens, T., 1994, The use of velocity spectrum for stacking receiver functions and imaging upper mantle discontinuities: Geophysical Journal International, v. 117, p. 427–440.

Hansen, W.R., 1984, Post-Laramide tectonic history of the eastern Uinta Mountains, Utah, Colorado, and Wyoming: The Mountain Geologist, v. 21, p. 5–29.

Karlstrom, K.E., and Houston, R.S., 1984, The Cheyenne belt: Analysis of a Proterozoic suture in southern Wyoming: Precambrian Research, v. 25, p. 415–446.

Karlstrom, K.E., and Humphreys, E.D., 1999, Persistent influence of Proterozoic accretionary boundaries in the tectonic evolution of southwestern North America: Interaction of cratonic grain and mantle modification events: Laramie, University of Wyoming, p. 161–179.

Keller, G.R., Snelson, C.M., Sheehan, A.F., and Dueker, K.G., 1998, Geophysical studies of crustal structure in the Rocky Mountain region: A review: Rocky Mountain Geology, v. 33, p. 217–228.

Langston, C.A., 1977, The effect of planar dipping structure on source and receiver responses for constant ray parameter: Seismological Society of America Bulletin, v. 67, p. 1029–1050.

Langston, C.A., and Hammer, J.K., 2001, The vertical component P-wave receiver function: Seismological Society of America Bulletin, v. 91, p. 1805–1819.

Lowry, A.R., and Smith, R.B., 1995, Strength and rheology of the western U.S. Cordillera: Journal of Geophysical Research, v. 100, p. 17,947–17,963.

Park, J., and Levin, V., 2000, Receiver functions from multiple-taper spectral correlation estimates: Seismological Society of America Bulletin, v. 90, p. 1507–1520.

Poppeliers, C.J., 2000, Imaging the Cheyenne belt: Three dimensional plane wave migration of P-to-S converted phases: Eos (Transactions, American Geophysical Union), v. 81.

Sheehan, A.F., Abers, G.A., Jones, C.H., and Lerner-Lam, A.L., 1995, Crustal thickness variations across the Colorado Rocky Mountains from teleseismic receiver functions: Journal of Geophysical Research, v. 100, p. 20,391–20,404.

Sheehan, A.F., Shearer, P.M., Gilbert, H.J., and Dueker, K.G., 2000, Seismic migration processing of P-SV converted phases for mantle discontinuity structure beneath the Snake River Plain, western United States: Journal of Geophysical Research, v. 105, p. 19,055–19,065.

Simpson, R.W., Jachens, R.C., Blakely, R.J., and Saltus, R.W., 1986, A new isostatic residual gravity map of the conterminous United States with a discussion on the significance of isostatic residual anomalies: Journal of Geophysical Research, v. 91, p. 8348–8372.

Snelson, C.M., Henstock, T.J., Keller, G.R., Miller, K.C., and Levander, A., 1998, Crustal and uppermost mantle structure along the Deep Probe seismic profile: Detection of waves converted from P to SV in the mantle: Rocky Mountain Geology, v. 33, p. 181–198.

Thouvenot, F., Kashubin, S.N., Poupinet, G., Makovskiy, V.V., Kashubina, T.V., Matte, P., and Jenatton, L., 1995, The root of the Urals: Evidence from wide-angle reflection seismics: Tectonophysics, v. 250, p. 1–13.

Vinnik, L.P., 1977, Detection of waves converted from P to SV in the mantle: Physics of the Earth and Planetary Interiors, v. 15, p. 39–45.

Wilson, J.T., 1966, Did the Atlantic close and then re-open?: Nature, v. 211, p. 676–681.

Woodward, L.A., 1988, Tectonic map of the Rocky Mountain region of the United States, *in* Sloss, L.L., ed., Sedimentary cover—North American Craton: Boulder, Colorado, Geological Society of America, Geology of North America, v. D-2, plate 2.

Zhu, L., and Kanamori, H., 2000, Moho depth variation in southern California from teleseismic receiver functions: Journal of Geophysical Research, v. 105, p. 2969–2980.



Manuscript received 31 January 2003
Revised manuscript received 23 April 2003
Manuscript accepted 25 April 2003

Printed in USA